Hydrogen Bond Compression during Triple Proton Transfer in Crystalline Pyrazoles. A Dynamic ^{15}N NMR Study

OLIVER KLEIN,[a] MARIA MINGUET BONVEHI,[a] FRANCISCO AGUILAR-PARRILLA,[a,†] NADINE JAGEROVIC,[b] JOSÉ ELGUERO,[b] AND HANS-HEINRICH LIMBACH[a,*]

[a]Fachbereich Biologie, Chemie und Pharmazie, Freie Universität Berlin, Takustrasse 3, D-14195 Berlin, Germany

[b]Instituto de Química Médica, Consejo Superior de Investigacíones Científicas (CSIC), Juan de la Cierva 3, E-28006 Madrid, Spain

(Received 11 February 1999 and in revised form 13 June 1999)

Abstract. Using dynamic solid state ^{15}N CPMAS NMR spectroscopy (CP ≡ cross polarization, MAS ≡ magic-angle spinning), the kinetics of degenerate intermolecular triple proton and deuteron transfers in the cyclic trimers of ^{15}N-labeled polycrystalline 4-nitropyrazole ($4NO_2P$) and 4-bromopyrazole (4BrP) have been studied as a function of temperature and are compared to the kinetics of triple proton transfer in bulk solid 3,5-dimethylpyrazole (DMP) studied previously. The results show that the transfer kinetics in the new trimers are much faster than in DMP. However, the kinetic HHH/HHD/HDD/DDD isotope effects of $4NO_2P$ are similar to those of DMP. These effects indicate a single barrier for the triple proton transfers where all three protons lose zero-point energy in the transition state, as expected for a structure with three compressed hydrogen bonds. At low temperatures, strong deviations from an Arrhenius-behavior are observed which are described in terms of a modified Bell tunneling model and a concerted proton motion. The barrier for the triple proton transfer in $4NO_2P$ and 4BrP is substantially smaller than in DMP. As there is no correlation with the electronic properties of the substituents, we assign this finding to steric effects where the bulky methyl groups of DMP in the 3- and 5-positions hinder the hydrogen bond compression, in contrast to $4NO_2P$ and 4BrP exhibiting substitutents in the 4-position. These results lead to a minimum energy pathway of the proton transfer following in the absence of steric hindering the hydrogen bond correlation line $q_1 = f(q_2)$, established previously, where q_1 represents the deviation of the proton from the hydrogen bond center and q_2 the N...N distance. Tunneling occurs at constant N...N distances.

INTRODUCTION

Because of the complexity of the phenomenon of proton transfer in water, there has been a constant effort in recent years to define and to study intermolecular[1–7] and intramolecular[1,8–10] multiple proton transfers in model systems using dynamic NMR spectroscopy. In addition, kinetic isotope effects were also determined and modeled. For example, H/D/T isotope effects were reported for single proton transfer in the porphyrin anion;[10] for several intramolecular[8,9b,9d] and intermolecular[6,7] double proton transfers the kinetic HH/HD/DD isotope effects could be obtained. From the interpretation of these effects it follows that intramolecular transfers are generally stepwise processes.[8–10] The intermolecular transfer reactions[6] were interpreted in terms of concerted proton motions, assisted by hydrogen bond compression. Tunneling through the barrier[11] was found to be important in nearly all cases.

Particularly interesting is a series of pyrazoles[2–5] because in the crystalline state they can form various

*Author to whom correspondence should be addressed.
E-mail: limbach@chemie.fu-berlin.de
†Present address: Schering AG, D-13342 Berlin, Germany

This paper was presented at the Research Workshop of the Israel Science Foundation: Proton Solvation and Proton Mobility, Neve Ilan, Israel, 18–22 October 1998.

hydrogen-bonded superstructures such as chains, helices, and cyclic hydrogen-bonded dimers, trimers, and tetramers. The latter exhibit double, triple, or quadruple proton transfers,[2a,2c] as demonstrated by various NMR methods. The first, and best-studied, case is 3,5-dimethylpyrazole (DMP, Fig. 1) which forms cyclic trimers in the solid state, for which a degenerate triple proton transfer was reported by Elguero et al.[2a] using high-resolution solid-state ^{13}C CPMAS NMR (CP ≡ cross polarization, MAS ≡ magic-angle spinning). Partial rate constants and kinetic isotope effects obtained by ^{15}N CPMAS NMR line shape analysis were reported in ref 2b. However, only recently the full kinetic HHH/HHD/HDD/DDD isotope effects of this process could be obtained in a wide temperature range by application of ^{15}N CPMAS NMR line shape analysis and a magnetization transfer experiment.[5] The results indicated a concerted triple hydron transfer mechanism proceeding at low temperatures by tunneling. (Hydron is the general term for the proton, deuteron, and triton.) At high temperatures, it was postulated that the proton transfer is assisted by hydrogen bond compression, as predicted by ab initio calculations.[4]

The present study was initiated in order to study in more detail the dependence of the kinetics of triple proton transfer in this type of compounds as a function of their chemical structure. The difficulty was that changing the substituents normally also changes the hydrogen-bonded structure in the solid state. However, recently the crystal structures of two other pyrazoles, 4-nitropyrazole ($4NO_2P$)[2d] and 4-bromopyrazole (4BrP)[2g] (Fig. 1), were solved, showing that both molecules formed cyclic trimers like that of DMP. The compounds exhibit all the typical signs of a static or dynamic proton disorder with half hydrogen atom density on all nitrogen atoms corresponding to the tautomeric processes depicted in Fig. 1. These findings motivated us to perform the NMR study presented in this paper, where we show by ^{15}N CPMAS NMR of the doubly ^{15}N-labeled compounds $4NO_2P$ and 4BrP that both exhibit a degenerate solid state triple proton transfer similar to that of DMP. However, surprisingly, the transfer is much faster in $4NO_2P$ and 4BrP as compared to DMP. In order to know whether the smaller proton transfer barrier also leads to different multiple kinetic isotope effects, we measured these effects for $4NO_2P$ reported below, providing evi-

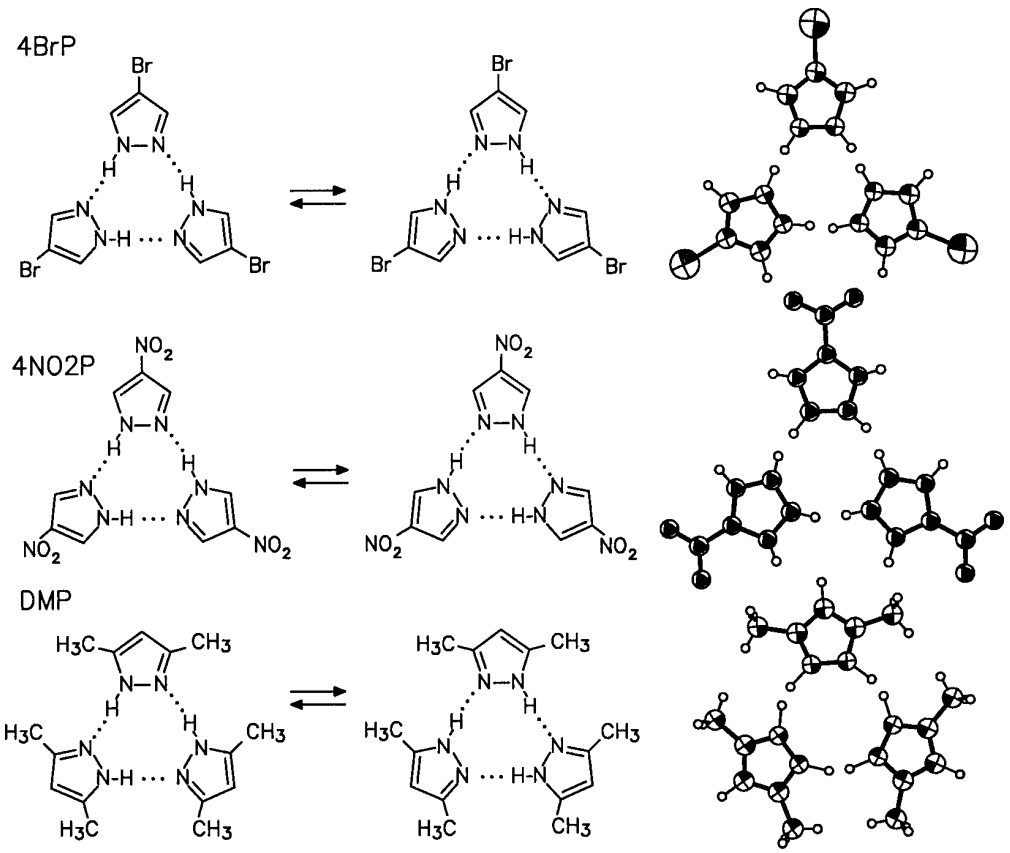

Fig. 1. Triple proton transfers in hydrogen-bonded cyclic trimers of crystalline 4BrP, $4NO_2P$, and DMP and including their crystal structures according to refs 2a,d,g.

dence for tunneling as in the case of DMP. We will assign the different proton transfer properties of the three compounds to the effect of substitution in the 3(5)-positions leading to steric hindrance for the compression of the hydrogen bonds during the proton transfer, in contrast to substitution in the 4-position.

The paper is organized as follows: after an experimental section, we present the results of the dynamic NMR experiments used as a tool to study the multiple proton transfer of the three trimers in the solid state. On the basis of these results, the differences in the dynamics of the proton processes are then discussed and explained by a simple steric model.

EXPERIMENTAL SECTION

The $^{15}N_2$-labeled compounds were synthesized according to procedures reported in the literature for the non-labeled compounds.[12,13] The desired deuterium fractions x_D for DMP and 4NO2P in the mobile proton sites were achieved by mixing CH_3OD as deuterating agent and CH_3OH in the corresponding amounts under argon atmosphere, followed by evaporation of the solvent in vacuo.

The ^{15}N CPMAS-NMR experiments were performed using Bruker MSL 300 (7 T), 300.13 MHz for ^1H and 30.41 MHz for ^{15}N and a 7 mm Doty standard high-speed CPMAS probe and a Bruker CXP 90 (2.1 T), 90.02 MHz for ^1H and 9.12 MHz for ^{15}N equipped with a 7 mm Doty standard probe. For both spectrometers, spinning speeds were so high (3–7 kHz) that rotational side bands could be mostly avoided. Because of sample heating in the case of the high-speed probe,[14a] a small quantity of ^{15}N-labeled tetramethyl-tetraaza-[14]-annulene (TTAA) was added in a separate capsule into rotors in order to obtain the sample temperatures from the temperature-dependent ^{15}N chemical shifts of TTAA.[14b] On both spectrometers, a Bruker B-VT-1000 temperature unit was used to control the temperature of the bearing gas stream and a homebuilt heat exchanger to achieve low temperatures. Throughout this study, pure nitrogen was used as bearing and driving gas. All chemical shifts are related to external solid $^{15}NH_4Cl$ and given with an error of ±0.3 ppm.

Standard CPMAS spectra were measured using the usual CP pulse sequence[15] and the line-shape analyses done as described previously.[5]

RESULTS

In this section, we report the results of the dynamic ^{15}N CPMAS-NMR experiments performed on polycrystalline $4NO_2P$ and 4BrP as a function of temperature.

The rate constants k^{HHH} of the triple proton transfer processes in polycrystalline $4NO_2P$ and 4BrP were determined by line-shape analysis of the ^{15}N CPMAS-NMR spectra measured at different temperatures, at resonance frequencies of either 9.12 and/or 30.41 MHz. Some typical superposed experimental and theoretical spectra are depicted in Fig. 2, together with spectra reported previously.[2c,5] In all cases, two sharp signals are observed for the amino- (-NH-) and the imino- (-N=) nitrogen atom sites (see Table 1). As the cross-polarization dynamics of nuclei in different chemical sites are different,[16] which can lead to signal intensity distortions in the resulting spectra, the cross-polarization times t_{CP} used in the experiments were adjusted in such a way that the signals of the amino and imino nitrogen atom sites were equal. Small differences are also averaged out by magnetization transfer arising from the proton tautomerism.[5,17] As temperature is increased, the lines broaden and coalesce. At higher temperatures, only one fairly sharp line is observed. The observation that the coalesced line appears midway between the two low-temperature signals indicates that all nitrogen atoms are characterized, within the margin of error, by the same proton density of 0.5, i.e., that the equilibrium constant of the double proton transfer $K = 1$. The rate constants were determined by line-shape analysis using the usual two-site theory.[1,5] The agreement between the experimental and calculated spectra is very satisfactory.

The multiple kinetic HHH/HHD/HDD/DDD isotope effects on the triple proton transfer in $4NO_2P$ were obtained in a way similar to that described previously[5] for the case of DMP by line-shape analysis of the ^{15}N CPMAS spectra of the partially deuterated compound. k^{HHD} was obtained from a sample exhibiting a deuteron fraction in the mobile sites of $x_D = 0.2$ after the previous determination of k^{HHH} at $x_D = 0$, and k^{DDD} from a sample with $x_D = 0.8$ after the previous determination of k^{DDD} from a sample with $x_D = 0.95$. All obtained rate constants and the resulting isotope effects are collected in Tables 2 and 3. As we did not find large differences in the isotope effects between $4NO_2P$ and DMP, we did not study further these effects for the case of 4BrP. The dependence of the rate constants on temperature for the three compounds is depicted in the Arrhenius diagrams of Figs. 3–5. For a better comparison, we have included in Fig. 5 the Arrhenius curves of the triple proton and deuteron transfers in $4NO_2P$ and DMP as dashed and dotted lines.

Table 1. ^{15}N chemical shifts of N-H pyrazoles in the solid state

	δ(-N=)	δ(N-H)
DMP	241.3	166.8
$4NO_2P$	243.2	170.7
4BrP	247.0	172.3

Reference: solid $^{15}NH_4Cl$; ppm values are given with a margin of error of ±0.3 ppm.

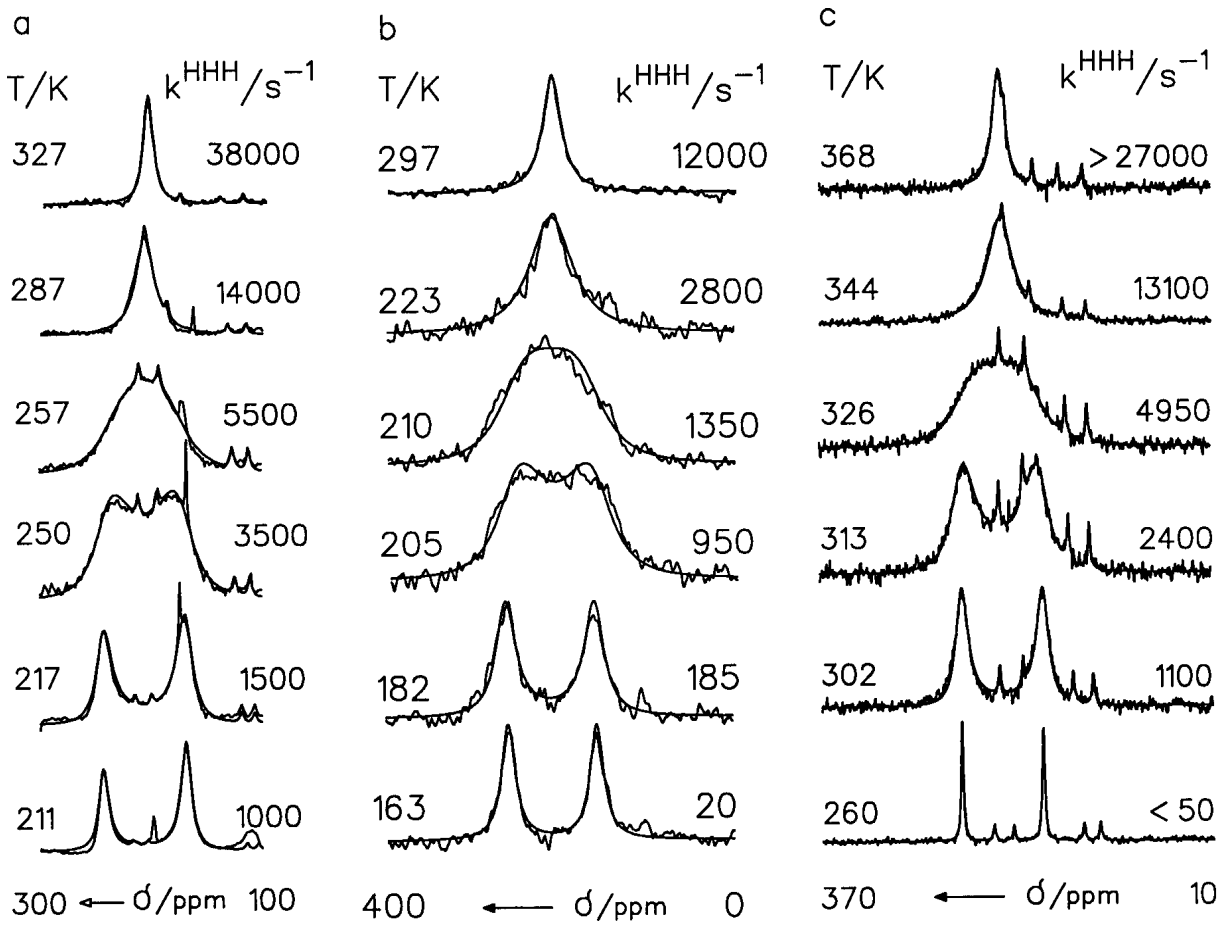

Fig. 2. Superposed experimental and calculated 9.12 MHz (4BrP) and 30.41 MHz (4NO_2P and DMP) ^{15}N CPMAS-NMR spectra of 95% ^{15}N-enriched 4BrP, 4NO_2P, and DMP as a function of temperature (Fig. 2a,b,c, respectively). The spectra of DMP were adapted from refs 2e and 5. Experimental conditions: 3–7 kHz sample spinning, 3–12 ms CP times, 4.3 s repetition time, 5–7 μs ^{1}H 90° pulses. The four sharp lines at the 30.41 MHz spectra with temperature-dependent line positions stem from a small quantity of ^{15}N-labeled tetramethyltetraaza-[14]-annulene (TTAA) added in a separate capsule. The line positions directly calibrate the internal temperature of the sample inside the rotor.[15]

Table 2. Rate constants of proton transfer in polycrystalline 4BrP and 4NO_2P obtained by ^{15}N CPMAS-NMR line-shape analysis

4BrP		4NO_2P							
T/K	k^{HHH}/s^{-1}	T/K	k^{HHH}/s^{-1}	T/K	k^{HHD}/s^{-1}	T/K	k^{HDD}/s^{-1}	T/K	k^{DDD}/s^{-1}
211	750	143	<10	262	3160	295	7000	251	140
223	1000	163	~20	252	2000	285	4500	256	170
229	1500	182	185	242	1500	280	4000	265	300
238	1700	192	360	237	750	273	3500	273	650
241	2600	200	670	233	400	269	3000	276	890
243	3000	205	950	220	400			280	1150
250	3500	210	1350					286	2100
254	4500	223	2800					297	3000
257	5500	239	>5000						
263	7000	239	>10000						
267	8500								
271	≈11000								

4NO_2P: doubly ^{15}N-labeled compound, experiments performed at 9.12 MHz and 30.41 MHz. 4BrP: doubly ^{15}N-labeled compound, experiments performed at 30.41 MHz.

Table 3. Rate constants and kinetic isotope effects of the triple hydron transfer in polycrystalline DMP, $4NO_2P$, and 4BrP at 300 K

DMP				$4NO_2P$				4BrP	
k^{HHH}/s^{-1}	1016	k^{HHH}/k^{DDD}	47	k^{HHH}/s^{-1}	21400[a]	k^{HHH}/k^{DDD}	29	k^{HHH}/s^{-1}	8800[a]
k^{HHD}/s^{-1}	270.5	k^{HHH}/k^{HHD}	3.8	k^{HHD}/s^{-1}	63200[a]	k^{HHH}/k^{HHD}	3.4		
k^{HDD}/s^{-1}	73.5	k^{HHD}/k^{HDD}	3.7	k^{HDD}/s^{-1}	20200[a]	k^{HHD}/k^{HDD}	3.1		
k^{DDD}/s^{-1}	21.6	k^{HDD}/k^{DDD}	3.4	k^{DDD}/s^{-1}	7500[a]	k^{HDD}/k^{DDD}	2.7		

[a]Values extrapolated to 300 K from the experimental low-temperature data, using the modified Bell tunneling model.

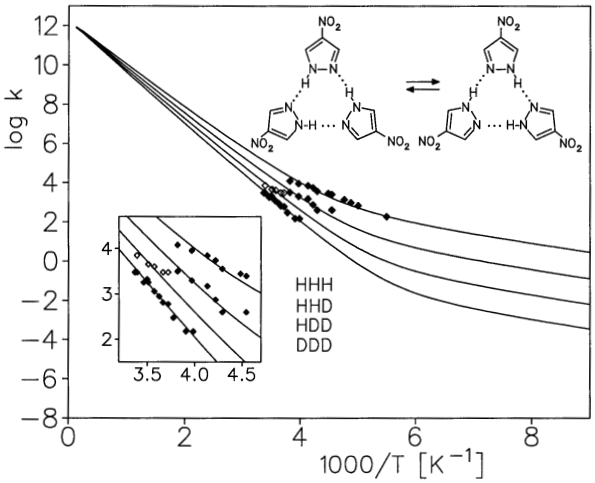

Fig. 3. Arrhenius diagram for triple proton and deuteron transfer in solid $4NO_2P$. The solid curves were calculated using a modified Bell tunneling model, as described in the text.

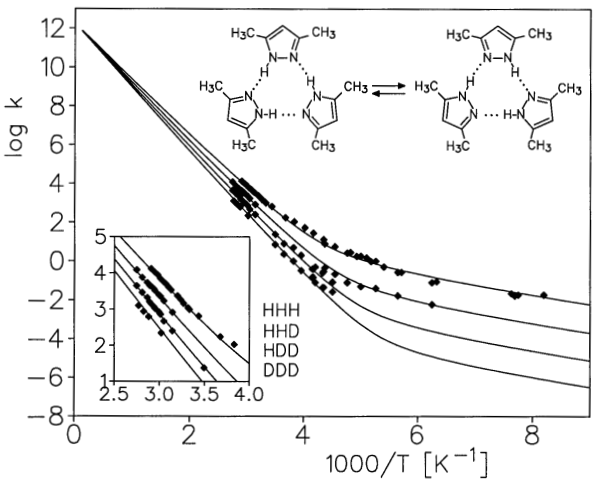

Fig. 4. Arrhenius diagram for the triple proton and deuteron transfer in solid DMP. The solid curves were calculated using a modified Bell tunneling model, as described in the text. Adapted from ref 5.

DISCUSSION

The main information from the Arrhenius diagrams of Figs. 3 to 5 is the following: (i) all three molecules—DMP, $4NO_2P$, and 4BrP—form cyclic trimers in the solid state exhibiting degenerate triple proton transfers; (ii) the proton transfer barriers in $4NO_2P$ and 4BrP are substantially smaller as compared to DMP; (iii) the multiple kinetic isotope effects $k^{HHH}/k^{DHH} \approx k^{DHH}/k^{DDH} \approx k^{DDH}/k^{DDD}$ are similar in DMP and $4NO_2P$ and follow the rule of the geometric mean (RGM) at high temperatures; (iv) at low temperatures the Arrhenius curves show a concave curvature leading to deviations of $k^{HHH}/k^{DHH} \approx k^{DHH}/k^{DDH} \approx k^{DDH}/k^{DDD}$ from the RGM, indicating that the reaction takes place in a dominant way by tunneling.

The high-temperature kinetic isotope effects k^{HHH}/k^{HHD}, k^{HHD}/k^{HDD}, and k^{HDD}/k^{DDD} can be ascribed to the loss of a similar zero-point energy $\Delta\varepsilon$ of each hydron in the transition state, as depicted in Fig. 6 for a single-barrier case involving a concerted proton motion; different effects would be observed in the case of a stepwise proton motion.[5] The deviations of these isotope effects from the RGM can be reproduced in terms of a modified Bell tunneling model[5,9] leading to the calculated lines of

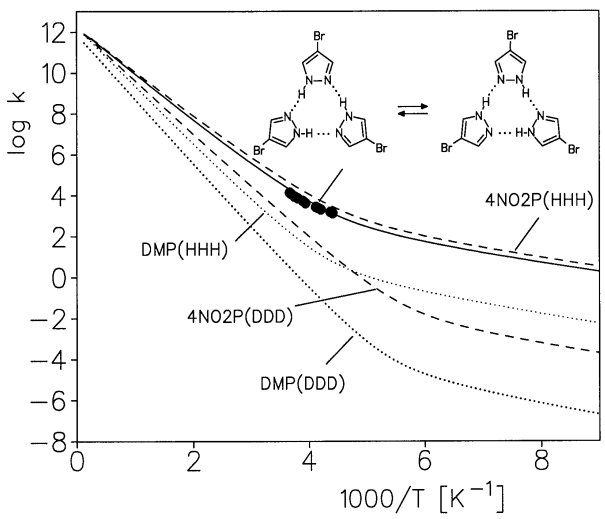

Fig. 5. Arrhenius diagram for triple proton transfer in solid 4BrP. The solid line was calculated using a modified Bell tunneling model, as described in the text. For comparison, the Arrhenius curves of triple proton and deuteron transfers in $4NO_2P$ and DMP are included as dashed and dotted lines, respectively.

Figs. 3 to 5. These curves depend on the following parameters:

(i) $E_m = E_r + E_i$ represents a minimum energy for tunneling to occur, and is assumed to be isotope-independent. E_r represents a contribution arising from heavy-atom reorganization *preceding* the hydron tunneling process at $T = 0$. E_i represents the energy of a possible intermediate and is zero in the single barrier case.

(ii) E_d^{HHH} is the barrier height for the triple proton transfer; it does not include E_m.

(iii) $\Delta\varepsilon$ represents the increase of the barrier height by replacing a single H by D. For a concerted process $\Delta\varepsilon = E_d^{HHD} - E_d^{HHH} = E_d^{HDD} - E_d^{HHD} = E_d^{DDD} - E_d^{HDD}$. This assumption is responsible for the validity of the RGM at high temperatures.

(iv) $2a$ is the barrier width of the H transfer in angstroms at the energy E_m.

(v) A single frequency factor A (in s^{-1}) is used for all isotopic reactions, i.e., a possible mass dependence[9] is neglected within the margin of error.

(vi) The tunneling masses are given in the stepwise case by $m_{eff}^{L} = m^{L} + \Delta m$, L = H, D, and in the concerted case by $m_{eff}^{LLL} = m^{LLL} + \Delta m$, with the fixed values $m^{H} = 1$, $m^{D} = 2$, $m^{HHH} = 3$, $m^{HHD} = 4$, $m^{HDD} = 5$, $m^{DDD} = 6$. Δm takes into account the possibility of small heavy-atom displacements during the tunnel process.

The agreement between experimental and calculated rate constants in Figs. 3–5 is satisfactory. The parameters obtained are collected in Table 4. As the Arrhenius diagram of DMP contained the largest number of rate constants, we have first fitted the solid lines of Fig. 4 to the experimental data. For the calculation of the two other Arrhenius diagrams, we then only varied E_d, E_m, and $2a$. Whereas E_m is similar for all compounds, E_d and $2a$ are smaller for $4NO_2P$ and 4BrP, resulting in faster proton transfer kinetics. Nevertheless, the physical significance of the barrier parameters should not be overestimated, in view of the many approximations used in this model. Noteworthy is the additional tunneling mass of $\Delta m = 2.7$ which indicates a substantial heavy-atom tunneling contribution. This contribution could arise either from the reorganization of the pyrazole skeleton or from a small-angle reorientation of the whole pyrazole molecules *during* the hydron tunnel process.

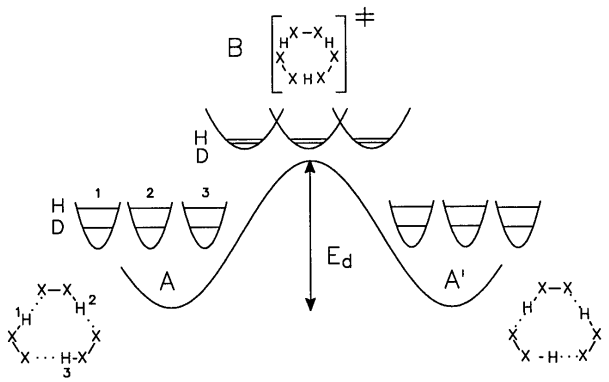

Fig. 6. One-dimensional reaction energy profile (schematically) for a degenerate single-barrier (concerted) triple-hydron transfer.

The finding of a smaller proton transfer barrier in $4NO_2P$ and 4BrP does not correlate with the normal substituent effect. The electron-withdrawing nitro group enhances the acidity of the NH group, and decreases the basicity of the non-protonated nitrogen, as indicated by the pK_a values of DMP, $4NO_2P$, and 4BrP included in Table 4.[2h] However, for degenerate triple proton transfer, this electronic effect is cancelled as an increase of the acidity of the protonated nitrogen group is matched by the decrease of the basicity of the non-protonated nitrogen. Thus, both electronic effects cancel, i.e., are not responsible for the different proton tranfer kinetics in this series of compounds, and both $4NO_2P$ and 4BrP exhibit similar proton transfer barriers. In other words, from this standpoint, there is no reason that the DMP should exhibit a larger barrier of proton transfer.

However, the DMP molecule contains bulky methyl groups in the 3- and 5-positions, that can exhibit steric effects. Thus, we assign the longer intermolecular N...N distance in this molecule (Table 4) to this steric effect. If we assume a hydrogen-bond-compression-assisted proton-transfer mechanism as proposed in ref 5 for DMP, by which the N...N distances are substantially reduced in the transition state, the higher barrier for the latter as compared to $4NO_2P$ and 4BrP becomes immediately clear, as illustrated in Fig. 7. Because of the bulky methyl groups, the hydrogen-bond compression is hindered, as compared to the molecules which are substituted only in the 4-position.

In order to discuss in further detail this hydrogen bond compression mechanism, we refer to the concept of Pauling[18a] and Brown[18b] to associate empirically to any bond between two atoms i and j a valence bond order p_{ij} which decays exponentially with the bond distance r_{ij}, i.e.,

$$p_{ij} = \exp[-(r_{ij} - r_{ij}^{o}) / b_{ij}] \qquad (1)$$

This concept has been used by Dunitz[18c] in order to map pathways of chemical reactions using a series of crystallographic structures. It has been applied by Truhlar[19a] and Agmon[19b] in order to simplify the theoretical description of gas-phase reactions.

Table 4. Molecular and dynamic properties of DMP $4NO_2$, 4BrP

	space group	r_{NN}/Å	pK_{a1}	pK_{a2}	E_d	E_m	Δε	log A	Δm	2a/Å
DMP	$R\,\bar{3}c$	2.98	4.06	15.00	48.1	8.4	2.7	12.3	2.8	0.43
$4NO_2P$	$P\,\bar{1}$	2.87	–2.00	9.64	36.0	7.52	2.7	12.3	2.8	0.39
4BrP	Pnma	2.89	0.63	12.69	38.0	7.53	2.7	12.3	2.8	0.39

pK_{a1}: values for the equilibrium pyrazolium/pyrazole in water and pK_{a2}: values of the equilibrium pyrazole/pyrazole anion.[2h] Parameters of the modified Bell tunneling model: barrier height E_d and minimum energy for tunneling E_m in kJ mol^{-1}, Δε additional barrier energy for replacing one H by D in kJ mol^{-1}, barrier width 2a in Å, frequency factor A (in s^{-1}). (Tunneling masses $m_{eff}^{LLL} = m^{LLL} + \Delta m$, $m^{HHH} = 3$, $m^{HHD} = 4$, $m^{HDD} = 5$, $m^{DDD} = 6$). Due to an error, the parameters of the tunneling process in DMP reported previously in ref 5 were not those corresponding to the calculated Arrhenius curves in fig. 9 of ref 5. The correct parameters used are listed in this Table.

Within this concept there is no principal difference between the "covalent" A–H and the "hydrogen bond" H···B, besides different valence bond orders and bond distances. As the total valency of hydrogen is unity, i.e.,

$$p_{AH} + p_{HB} = 1 \qquad (2)$$

it follows that the two bond distances r_{AH} and r_{HB} of a hydrogen bond cannot be varied independently, a consequence which has been verified by crystallography by several authors[20] for a number of hydrogen-bonded systems. Limbach and coworkers have verified this correlation recently from a theoretical standpoint and by solid state NMR.[21] In addition, several other hydrogen-bond properties such as geometric H/D isotope effects, zero-point energy changes, and chemical shifts could be modeled in terms of the valence bond order concept.[21]

This hydrogen-bond correlation can conveniently be written in terms of the coordinates

$$q_2 = 2r_0 + 2q_1 + 2b \ln[1 + \exp\{-2q_1/b\}],$$
$$b = 0.404 \text{ Å, and } r_0 = 0.99 \text{ Å} \qquad (3)$$

where $q_1 = \frac{1}{2}(r_1 - r_2)$ and $q_2 = r_1 + r_2$. In the case of a linear hydrogen bond, q_1 corresponds to the displacement of the proton from the hydrogen-bond center and q_2 to the heavy-atom distance. Equation 1 is depicted in Fig. 8, where we have included the experimental points for the three compounds studied here. Assuming linear hydrogen bonds, we obtain the NH-distances of 1.01 Å for DMP and 1.025 Å for the two other compounds. From eq 3 and the solid line in Fig. 8, it follows that if a proton is shifted towards the hydrogen-bond center that the N···N-distance strongly contracts. Apparently, all three hydrogen bonds are "cooperative" in the sense that the contraction of the first bond also leads to a contraction of the second and the third hydrogen bond, shifting the second and third proton equally to the hydrogen-bond center. Hence, a concerted proton motion results. We note that in several cases of intramolecular double-proton transfer systems,[8,9] a cooperative compression of both hydrogen bonds involved was not possible because of constraints arising from the molecular backbone, resulting in a stepwise proton transfer.

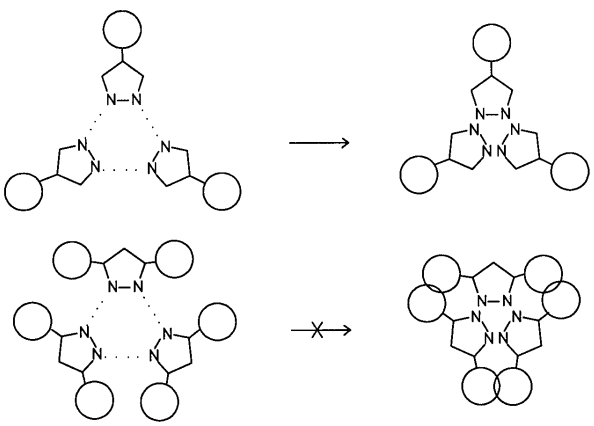

Fig. 7. Steric effects of substitution in the 3,5 and 4-position of pyrazoles on the hydrogen-bond-compression-assisted triple-proton transfer.

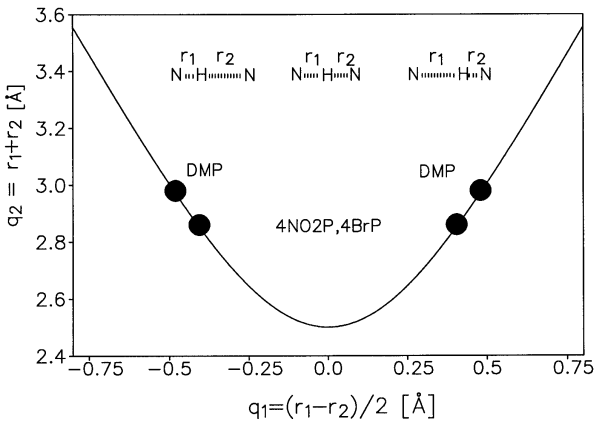

Fig. 8. Hydrogen-bond correlation according to ref 21 for the N–H···N hydrogen bonds of DMP, 4BrP, and $4NO_2P$. $q_1 = \frac{1}{2}(r_1 - r_2)$ represents the distance of the proton from the hydrogen-bond center, and $q_2 = r_1 + r_2$ represents the intermolecular N...N distance if the hydrogen bonds are linear.

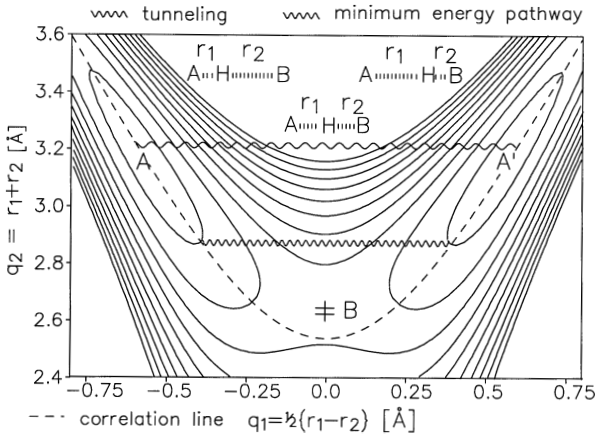

Fig. 9. Two-dimensional energy reaction surface involving a reduction of the all heavy atom distances $r_{N...N}$ prior to the hydron transfer, as proposed by ab initio calculations.[4] Points A and A′ correspond to the initial and final states of Fig. 6, and B corresponds to the transition state where the zero-point energies of all hydrons are reduced as indicated in Fig. 6. The minimum energy pathway (dashed curve) involves a substantial hydrogen-bond compression and an associated gradual shift of the hydron.

A general reaction energy surface for a hydrogen-bond-compression-assisted proton transfer, valid either for a single proton or for a concerted motion of several protons was proposed in ref 6c. This surface is depicted in Fig. 9, together with the correlation curve of Fig. 6. In contrast to the case of pyrazoles, we have arbitrarily chosen the potential wells to be located at $q_2 \approx 3.2$ Å and $q_1 \approx 0.6$ Å. We note that the minimum energy pathway which was represented in Fig. 4 in one dimension will first follow the correlation line $q_2 = f(q_1)$ as far as possible until steric hindrance stops the hydrogen-bond compression. Then the proton must be transferred at a constant N···N-distance. Tunneling can occur at each N···N-distance; tunneling at larger distances will dominate at higher temperatures, and at shorter distances at lower temperatures. The pathway is then longer for DMP as compared to 4BrP and $4NO_2P$, and will, therefore, require a larger energy barrier for the proton transfer.

The one-dimensional modified Bell tunneling model used to explain the temperature dependence of the rate constants does not take the two- or even higher-dimensional minimum energy pathway into account. Especially the minimum energy for tunneling to occur may no longer be needed as parameters if the two-dimensional reaction pathway would be taken into account.

CONCLUSIONS

We have provided evidence that hydrogen-bond compression is an important feature of proton transfer, which leads—together with the cooperativity or anti-cooperativity of coupled hydrogen bonds—to either concerted or stepwise proton transfers. In the case of three compounds, it was shown that the barrier of proton transfer is affected by the ease to compress the hydrogen bonds involved, which is more difficult if bulky groups hinder this motion. The use of hydrogen-bond correlations observed by crystallography, NMR, and theoretical calculations can help to construct proper energy reaction surfaces of proton transfer and to close the theoretical gap between the simple one-dimensional Bell model of tunneling and quantum-mechanical models.

Acknowledgments. We thank the Deutsche Forschungsgemeinschaft, Bonn-Bad Godesberg; the European Community, Brussels; and the Fonds der Chemischen Industrie, Frankfurt for financial support.

REFERENCES AND NOTES

(1) Limbach, H.H.; Scherer, G.; Meschede, L.; Aguilar-Parrilla, F.; Wehrle, B.; Braun, J.; Hoelger, C.; Benedict, H.; Buntkowsky, G.; Fehlhammer, W.P.; Elguero, J.; Smith, J.A.S.; Chaudret, B. *NMR Studies of Elementary Steps of Hydrogen Transfer in Condensed Phases.* In *Ultrafast Reaction Dynamics and Solvent Effects;* Gauduel, Y.; Rossky, P.J., Eds.; American Institute of Physics: AIP Conference Proceedings 298, 1994, Part III, pp 225–239.

(2) (a) Baldy, A.; Elguero, J.; Faure, R.; Pierrot, M.; Vicent, E.J. *J. Am. Chem. Soc.* **1985**, *107*, 5290. (b) Smith, J.A.S.; Wehrle, B.; Aguilar-Parrilla, F.; Limbach, H.H.; Foces-Foces, M.C.; Cano, F.H.; Elguero, J.; Baldy, A.; Pierrot, M.; Khurshid, M.M.T.; Larcombe-McDouall, J.B. *J. Am. Chem. Soc.* **1989**, *111*, 7304. (c) Aguilar-Parrilla, F.; Scherer, G.; Limbach, H.H.; Foces-Foces, M.C.; Cano, F.H.; Smith, J.A.S.; Toiron, C.; Elguero, J. *J. Am. Chem. Soc.* **1992**, *114*, 9657. (d) Lamas-Saiz, A.L.; Foces-Foces, M.C.; Cano, F.H.; Jimenez, P.; Laynez, J.; Meutermans, W.; Elguero, J.; Limbach, H.H.; Aguilar-Parrilla, F. *Acta Crystallogr.* **1994**, *B50*, 746. (e) Aguilar-Parrilla, F.; Limbach, H.H.; Foces-Foces, M.C.; Cano, F.H.; Jagerovic, N.; Elguero, J. *J. Org. Chem.* **1995**, *60*, 1965. (f) Hoelger, C.; Limbach, H.H.; Aguilar-Parrilla, F.; Elguero, J.; Weintraub, O.; Vega, S. *J. Magn. Res.* **1996**, *A120*, 46. (g) Foces-Foces, M.C.; Llamas-Saiz, A.L.; Elguero, J. *Z. Kristallogr.* **1999**, *214*, 237. (h) Catalan, J.; Abboud, J.L.M.; Elguero, J. *Adv. Heterocycl. Chem.* **1987**, *41*, 187.

(3) (a) Toda, F.; Tanaka, K.; Foces-Foces, M.C.; Llamas-Saiz, A.; Limbach, H.H.; Aguilar-Parrilla, F.; Claramunt, R.M.; Lopez, C.; Elguero, J. *J. Chem. Soc., Chem. Commun.* 1993, 1139. (b) Aguilar-Parrilla, F.; Claramunt, R.M.; Lopez, C.; Sanz, D.; Limbach, H.H.; Elguero J. *J. Phys. Chem.* **1994**, *98*, 8752.

(4) de Paz, J.L.G.; Elguero, J.; Foces-Foces, M.C.; Llamas-Saiz, A.; Aguilar-Parrilla, F.; Klein, O.; Limbach, H.H. *J. Chem. Soc., Perkin Trans. 2* **1997**, 101.
(5) Aguilar-Parrilla, F.; Klein, O.; Elguero, J.; Limbach, H.H. *Ber. Bunsen-Ges. Phys. Chem.* **1997**, *101*, 889.
(6) (a) Männle, F.; Wawer, I.; Limbach, H.H. *Chem. Phys. Lett.* **1996**, *256*, 657. (b) Anulewicz, R.; Wawer, I.; Krygowski, T.M.; Männle, F.; Limbach, H.H. *J. Am. Chem. Soc.* **1997**, *119*, 12223. (c) Meschede, L.; Limbach, H.H. *J. Phys. Chem.* **1991**, *95*, 10267.
(7) (a) Meyer, R.; Ernst, R.R. *J. Chem. Phys.* **1990**, *93*, 5518. (b) Stöckli, A.; Meier, B.H.; Kreis, R.; Meyer, R.; Ernst, R.R. *J. Chem. Phys.* **1990**, *93*, 1502. (c) Heuer, A.; Haeberlen, U. *J. Chem. Phys.* **1995**, *95*, 4201.
(8) Scherer, G.; Limbach, H.H. *J. Am. Chem. Soc.* **1994**, *116*, 1230 and references therein.
(9) (a) Wehrle, B.; Zimmermann, H.; Limbach, H.H. *J. Am. Chem. Soc.* **1988**, *110*, 7014. (b) Braun, J.; Schlabach, M.; Wehrle, B.; Köcher, M.; Vogel, E.; Limbach, H.H. *J. Am. Chem. Soc.* **1994,** *116*, 6593. (c) Hoelger, C.; Wehrle, B.; Benedict, H.; Limbach, H.H. *J. Phys. Chem.* **1994**, *98*, 843. (d) Braun, J.; Limbach, H.H.; Williams, P.G.; Morimoto, H.; Wemmer, D.E. *J. Am. Chem. Soc.* **1996**, *118*, 7231 and references therein.
(10) (a) Braun, J.; Schwesinger, R.; Williams, P.G.; Morimoto, H.; Wemmer, D.E.; Limbach, H.H. *J. Am. Chem. Soc.* **1996**, *118*, 11101. (b) Brackhagen, O.; Scheurer, C.; Meyer, R.; Limbach, H.H. *Ber. Bunsen-Ges. Phys. Chem.* **1998**, *102*, 303.
(11) (a) Bell, R.P. *The Tunnel Effect*, 2nd ed.; Chapman and Hall: London, 1980. (b) Caldin, E.; Gold, V. *Proton Transfer*; Chapman and Hall: London, 1975.
(12) Elguero, J.; Jacquier, R. *Bull. Soc. Chim. Fr.* 1966, 2832.
(13) Hüttel, R.; Büchele, F.; Jochum, P. *Chem. Ber.* **1955**, *88*, 1577.
(14) (a) Aguilar-Parrilla, F.; Wehrle, B.; Bräunling, H.; Limbach, H.H. *J. Magn. Reson.* **1990**, *87*, 592. (b) Wehrle, B.; Aguilar-Parrilla, F.; Limbach, H.H. *J. Magn. Reson.* **1990**, *87*, 584.
(15) Torchia, D. *J. Magn. Reson.* **1978,** *30,* 613.
(16) (a) Fyfe, C.A. *Solid State NMR for Chemists*; C. F. C. Press: Guelph, Ontario, 1983.
(17) Limbach, H.H.; Wehrle, B.; Schlabach, M.; Kendrick, R.D.; Yannoni, C.S. *J. Magn. Reson.* **1988,** *77,* 84.
(18) (a) Pauling, L. *J. Am. Chem. Soc.* **1947**, *69*, 542. (b) Brown, I.D. *Acta Crystallogr.* **1992**, *B48*, 553 and references therein. (c) Dunitz, J.D. *Philos. Trans. R. Soc. London* **1975**, *B 272*, 99.
(19) (a) Truhlar, D.G., *J. Am. Chem. Soc.* **1972***, 94,* 7854. (b) Agmon, N. *Chem. Phys. Lett.* **1977**, *45*, 343.
(20) (a) Gilli, P.; Bertolasi, V.; Ferretti, V; Gilli, G. *J. Am. Chem. Soc.* **1994**, *116*, 909. (b) Steiner, T.; Saenger, W. Acta Crystallogr. **1994**, *B50*, 348. (c) Steiner, T. *J. Chem. Soc. Chem. Comm.* **1995**, 1331. (d) Steiner, T. *J. Phys. Chem. A* **1998**, *102*, 7041.
(21) Benedict, H.; Limbach, H.H.; Wehlan, M.; Fehlhammer, W.P.; Golubev, N.S.; Janoschek, R. *J. Am. Chem. Soc.* **1998**, *120*, 2939.
(22) (a) Smirnov, S.M.; Golubev, N.S.; Denisov, G.S.; Benedict, H.; Schah-Mohammedi, P.; Limbach, H.H. *J. Am. Chem. Soc.* **1996**, *118*, 4094. (b) Shenderovich, I.; Smirnov, S.; Denisov, G.S.; Gindin, V.; Golubev, N.S.; Dunger, A.; Reibke, R.; Kirpekar, S.; Malkina, O.L.; Limbach, H.H. *Ber. Bunsen-Ges. Phys. Chem.* **1998**, *102*, 422. (c) Golubev, N.S.; Shenderovich, I.; Smirnov, S.M.; Denisov, G.S.; Limbach, H.H. *Chem.—Eur. J.* **1999**, *5*, 492.